AIAA JOURNAL
Vol. 44, No. 7, July 2006

Neural Networks for Inverse Problems Using Principal Component Analysis and Orthogonal Arrays

Yong Y. Kim* and Rakesh K. Kapania†
Virginia Polytechnic Institute and State University, Blacksburg, Virginia 24061

An obstacle in applying artificial neural networks (NNs) to system identification problems is that the dimension and the size of the training set for NNs can be too large to use them effectively in solving a problem with available computational resources. To overcome this obstacle, principal component analysis (PCA) can be used to reduce the dimension of the inputs for the NNs without impairing the integrity of data and orthogonal arrays (OAs) can be used to select a smaller number of training sets that can efficiently represent the given behavior system. NNs with PCA and OAs are used here in solving two parameter identification problems in two different fields. The first problem is identifying the location of damage in cantilever plates using the free vibration response of the structure. The free vibration response is simulated using the finite element method. The second problem is identifying an anomaly in an illuminated opaque homogeneous tissue using near-infrared light based on the simulation of the photon intensity and the photon mean time of flight in perfect and imperfect tissues using the finite element method.

Introduction

THE objective of this work is to apply neural networks (NNs) in solving the inverse problems of damage detection in the structural engineering and of optical medical imaging problem in the biomedical engineering. This work is continuation of the work presented previously.[1] Our work is unique in that we try to apply one method to two seemingly totally different fields and try to benefit from utilizing the experience obtained from two different fields. Identifying damage parameters in damage identification problems and identifying cross sectional properties in optical imaging problems both require solving a large number of complex direct problems to construct large training sets. The common problems in applying NNs to the two problems are that the dimension of the inputs for NNs can be too high for a quick training of the NN and that the number of direct problem, which needs to be solved to construct the training set, can also be too large to obtain meaningful solution with the computing resources available. Principal component analysis can be used to reduce the dimension of the input to an NN and orthogonal arrays can be used to reduce the size of the training set efficiently and to obtain reasonable results. Here, the effect of using principal component analysis (PCA) and orthogonal arrays (OAs) in solving two inverse problems using NNs has been studied.

In the damage identification problem, a locally damaged plate finite element model developed in NASTRAN® commercial finite element package was utilized to evaluate the use of PCA and OAs for NNs. The data used as inputs for NNs in identifying the location of the damage were the transient response data at number of locations of the damaged plates. NNs were able to map automatically this two-dimensional damage location parameter space and give the values of damage location, given the transient response of the damaged beam, instantaneously. The problem in utilizing the transient response data was that the dimension of the input was quite large, making the use of NN somewhat impractical because of the time needed in training NNs. Therefore, the use of PCA was considered to be a viable option to reduce the dimension of the inputs for NNs. On the other hand, the size of training sample has to be such that it can cover most of the possible variations in the parameters. This requires huge number of training sets to be selected and solved. Using OAs, we can efficiently choose the training data set to be selected and used. The experience in utilizing NNs with PCA in the damage identification problem was found to be very valuable in solving the optical imaging problem and vice versa.

Optical imaging is the methodology of using light in a narrow wavelength band in the near-infrared range (∼700–1000 nm) to transilluminate a light diffusive media such as a human tissue and to use the resulting measurements of intensity on the tissue boundary to reconstruct a map the internal optical properties. The main advantage of optical imaging is its capability of safely and portably measuring tissue functions to detect nonfunctioning cells, such as cancerous cells. It is known that to be able to observe the functioning of cells a continuous and noninvasive imaging method is required. Moreover, optical imaging has advantages over x rays, computed tomography scans, and positron emission tomography scans because of its portability and lower equipment cost as well.[2] The main idea of optical imaging is that light passes through the body in small amounts, carrying with it characteristics about the tissues through which it has passed. Based on these characteristics, optical images can be obtained by solving the inverse problem of light propagation. However, diffusive and scattering characteristics of near-infrared light when propagating in a tissue leads to a highly nonlinear inverse problem whose solution requires large amounts of computational time even for relatively coarse measurements if conventional methods are used.[3,4]

The application of NN may help reduce this computational time, thus making the use of optical imaging to determine the presence of an anomaly in a tissue a more viable approach. The process of solving this inverse problem consists of two parts. The first part entails solving the direct problem of the light diffusion equation to predict propagation of photons in a tissue. The second part, based on the solutions of the direct problem and the information observed in the detectors, entails obtaining an optical image by solving the inverse problem.

In our research, we have used a finite element method (FEM) program to solve the direct problem and have integrated this program, with NNs available in the Neural Network Toolbox in MATLAB® to identify the location of an anomaly using measurements of near-infrared light that has propagated through a human tissue and has gone through a high degree of both scattering and absorption.

Presented as Paper 2003-2002 at the AIAA/ASME/ASCE/AHS/ASC 44th Structures, Structural Dynamics, and Materials Conference, Norfolk, VA, 7–10 April 2003; received 5 May 2004; accepted for publication 21 August 2005.

*Graduate Assistant, Department of Aerospace and Ocean Engineering; currently Research Professor, Center for Healthcare Technology Development, Chonbuk National University, Jeonjusi, Jeonbuk 561-756, Republic of Korea.

†Professor, Department of Aerospace and Ocean Engineering and Director, Multidisciplinary Analysis and Design Center for Advanced Vehicles. Associate Fellow AIAA.

In applying NNs to this problem, one of the problems was the large size of the dimension of the inputs. The inputs calculated at the surface consisted of detector readings at number of detector locations for each source positioned at number of locations. For example, if there are 20 detectors and 20 light sources, the dimension of the inputs is 400. However, the input sets can be highly correlated to each other. Therefore, PCA was used to reduce the dimension of data.

In our previous work, we have used the calculation of the time-independent integrated photon intensity only. Here, we added the calculation of the photon mean time of flight (PMTF) using FEM in identifying anomaly in a homogenous tissue.

PCA

PCA is an algorithm of self-organized learning for NNs. PCA decomposes the data set to the principal components and reduces the dimension of the input. This method is most useful in the cases when the dimension of the input is large but the data are highly correlated to each other and the size of the useful content is limited. The procedure in performing PCA is as follows.[5,6]

Let $[H]_{M\times N}$ be an output composed of M sampling points and N output sets. The first step in PCA is normalizing the matrix. The mean value and the standard variance at each point can be calculated as

$$\bar{H}_i = \frac{1}{N}\sum_{j=1}^{N} h_{ij} \tag{1}$$

$$S_i^2 = \frac{1}{N}\sum_{j=1}^{N} (h_{ij} - \bar{H}_i)^2 \tag{2}$$

Then, the output matrix can be normalized for each point as

$$\tilde{h}_{ij} = (h_{ij} - \bar{H}_i)\big/ S_i\sqrt{N} \tag{3}$$

From the normalized output matrix, the correlation matrix is calculated as

$$[C]_{M\times M} = [\tilde{H}]_{M\times N}[\tilde{H}]^T_{N\times M} \tag{4}$$

The eigenvectors and eigenvalues of the correlation matrix are the principal components of the output matrix and can be calculated from $[C]\{\Psi_i\} = \lambda_i\{\Psi_i\}$, where λ_i is the ith eigenvalue and $\boldsymbol{\Psi}_i$ is ith eigenvector. The eigenvalues and eigenvectors are ordered in a way that the largest value of eigenvalue comes first.

The maximum variation from the mean is calculated as

$$J_v = \sum_{i=1}^{M} \lambda_i \tag{5}$$

When we select first P principal components to reconstruct the output matrix, the reconstruction error is

$$J_e = \sum_{i=1}^{M} \lambda_i - \sum_{i=1}^{P} \lambda_i = \sum_{i=P+1}^{M} \lambda_i \tag{6}$$

The relative reconstruction error in representing the system with P number of principal component can be calculated as

$$E = \left(\sum_{i=P+1}^{M} \lambda_i\right)\Big/\left(\sum_{i=1}^{M} \lambda_i\right) \tag{7}$$

The value of P can be determined so that the error is within desired level.

The projection of the response variation matrix $[\tilde{H}]_{M\times N}$ to the principal components is

$$[A]_{M\times N} = [\Psi]_{M\times M}\,[\tilde{H}]_{M\times N} \tag{8}$$

If we choose to select P number of the principal components, the projection of the response variation matrix is reduced to $[A]_{M\times P}$. This reduced response variation matrix is used as input for the NNs instead of the full output matrix.

The normalized output matrix restored back from the reduced response variation matrix can be calculated as

$$[\tilde{H}] \approx [A]_{M\times P}[\Psi]_{N\times P} \tag{9}$$

The output matrix is restored back from the normalized output matrix by

$$h_{ijR}(\omega) = S_i\sqrt{N}\tilde{h}_{ij}(\omega) + \bar{H}_i \tag{10}$$

OAs

OAs can be defined as a simplified method of putting together an experiment. In OAs, orthogonal means being balanced and not mixed, and in the context of experimental matrices, it means statistically independent.[7] OAs has been employed in number of different areas.[7–9] One of their successful applications has been in quality engineering.[8]

As an example, Fig. 1 shows an OA with seven factors, two levels, and strength two. When we pick the two columns from the array, the possible combinations are 00, 01, 10, and 11. In Fig. 1, for any two columns picked, the number of the occurrence of the possible combination is always same. The maximum possible runs, which is called full factorial, can be calculated as $2^7 = 128$. Minimum runs selected by the OA are (number of levels -1) $\times$ (number of factor) $+ 1 = (2-1)\times 7 + 1 = 8$. The advantage of the OA is the benefit of efficiency and simplicity. For our use in NNs, OAs were selected from an internet database of OAs for matching number of factors and levels. (Data available online at http://www.research.att.com/~njas/oadir/ [cited 13 May 2006].)

Damage Identification

Damage was identified in a cantilevered plate shown in Fig. 2. NASTRAN was used to build a finite element (FE) model and obtain dynamic response. The damages were represented as elements with reduced Young's modulus. To identify the location of damage, two properties of the dynamic behavior of the damaged plate were utilized. One was the transient displacement response, and the other

	1	2	3	4	5	6	7
1	0	0	0	0	0	0	0
2	1	0	1	0	1	0	1
3	0	1	1	0	0	1	1
4	1	1	0	0	1	1	0
5	0	0	0	1	1	1	1
6	1	0	1	1	0	1	0
7	0	1	1	1	1	0	0
8	1	1	0	1	0	0	1

Fig. 1 Example of an OA (7 factors, 2 levels, strength 2).

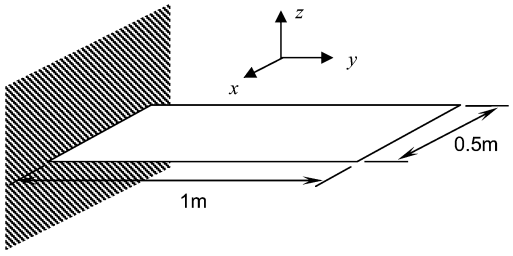

Fig. 2 Cantilever plate for damage identification problem, E = 62.05 GPa, ν = 0.35, ρ = 2700 kg/m^3, and thickness 5 mm.

was the frequency response function. To calculate the transient displacement response, NASTRAN was used to calculate modal stiffness and mode shapes of the plates repeatedly each with a damaged zone at different locations. Next, a mode superposition method was used to calculate transient response based on the transient input, the modal stiffness matrix, and the mode shapes of the plate for each case. PCA was used to reduce the dimension of the transient response before being used as input to NNs. To calculate the frequency response function, fast Fourier transform (FFT) was applied to the transient response obtained using the mode superposition method.

One of the problems in applying NNs to the damage identification problem was that we have to perform FE analysis for each damage location and feed the output file to the NNs' training and testing. Therefore, a code in MATLAB environment was developed that can automatically generate input file for NASTRAN for different locations of damage, execute the NASTRAN analysis for each case, read the modal data from the NASTRAN output file, and perform the mode superposition method and FFT. Next, the same code was used to train NNs and test the trained NNs. This procedure is shown in Fig. 3. This automatic code made it possible to generate training sets and testing sets, as many as needed, and to use the set directly in NN analysis.

To solve the dynamic equation (11), the reduced dynamic equation (12) was used, and this reduced dynamic equation was solved independently using piecewise linear approximation to obtain transient displacement response at various locations:

$$\boldsymbol{M}\ddot{\boldsymbol{u}} + \boldsymbol{K}\boldsymbol{u} = \boldsymbol{p}(t) \tag{11}$$

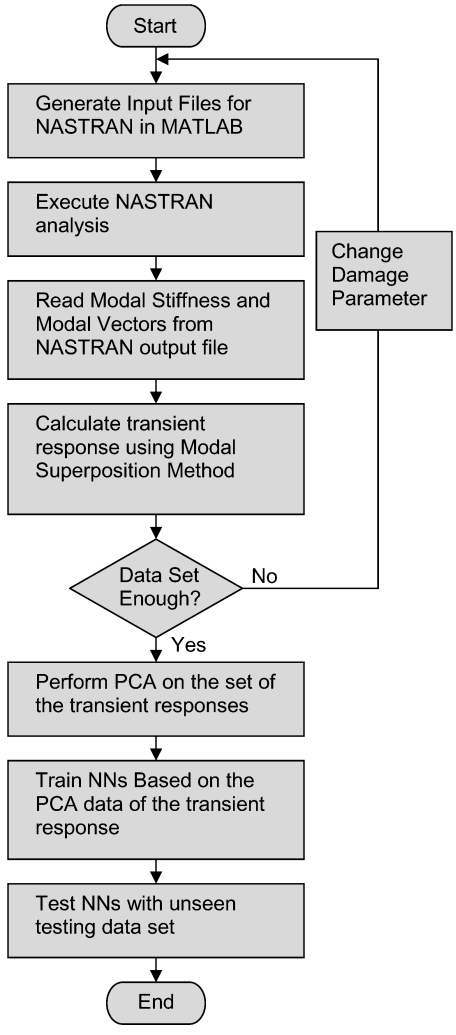

Fig. 3 Procedure for obtaining dynamic response and training and testing NNs.

$$\bar{\boldsymbol{M}}\ddot{\boldsymbol{\eta}} + \bar{\boldsymbol{K}}\boldsymbol{\eta} = \bar{\boldsymbol{p}}(t) \tag{12}$$

$$\boldsymbol{u} = \Phi\boldsymbol{\eta}, \qquad \bar{\boldsymbol{M}} = \Phi^t\boldsymbol{M}\Phi, \qquad \bar{\boldsymbol{K}} = \Phi^t\boldsymbol{K}\Phi, \qquad \bar{\boldsymbol{p}} = \Phi^t\boldsymbol{p}$$

where $\boldsymbol{M}$ is the mass matrix, $\boldsymbol{K}$ is the stiffness matrix, $\boldsymbol{p}(t)$ is the forced input vector, $\boldsymbol{u}$ is the displacement vector, $\bar{\boldsymbol{M}}$ is the modal stiffness matrix, $\bar{\boldsymbol{K}}$ is the modal stiffness matrix, $\bar{\boldsymbol{p}}$ is the modal force vector, $\boldsymbol{\eta}$ is the modal displacement vector, and Φ is the eigenvector matrix.

The FE model constructed for the damage identification has $40 \times 80 = 3200$ elements. The training set was selected for 10 locations in the x direction and 20 locations in the y direction. This resulted in 200 training sets. The testing set was selected at the midpoint between the training points. This resulted in $9 \times 19 = 173$ testing sets. For each set selected, modal stiffness and mode shapes were calculated using NASTRAN.

The transient out-of-plane response of the plate was calculated against the excitation by half-sine wave shown in Fig. 4. The transient responses were calculated at 8 locations using mode superposition method with 10 modes for each case. Figure 5 shows the location where the half-sine wave is applied and the locations where the transient displacement vectors were calculated.

The transient out-of-plane displacement vectors at eight locations were selected for the duration of 0.25 s and were arranged into one column of vectors for each training set. Next, PCA was applied to the transient displacement vector and the dimension reduced from 4000 to 44 when the relative error was set to be 0.1%.

An NN was trained with the reduced set of principal component of the displacement vector. The NN used was multilayer feedforward backpropagation NN. The resilient backpropagation training scheme was used. The targets were the x and y coordinates of the center of the damaged zone. The size of the training input matrix was 44×200, and that of the target was 2 by 200. The training took 24 s in a Sun Blade 1000 workstation to reach the simulation error goal. Figure 6 shows the simulation errors of trained NNs relative to the length of the plate. Here, we can see that simulation error is not more than 4% and not less than 2%.

Next, instead of the displacement data, FFT of the transient out-of-plane displacement vector was used as the training inputs for NNs.

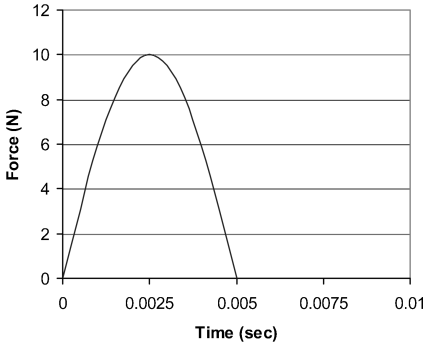

Fig. 4 Time history of force applied to plate.

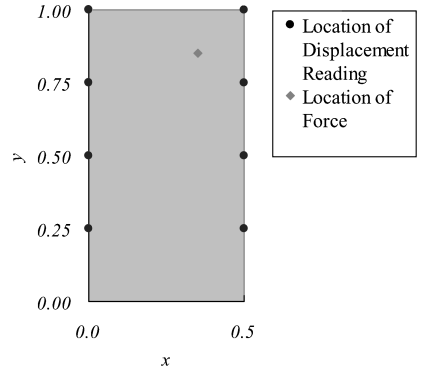

Fig. 5 Locations of displacement reading and force applied.

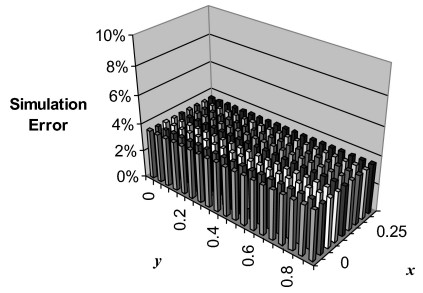

Fig. 6 Relative simulation error of NN trained with PCA of transient displacement vector at each testing point placed in midway between training data points in predicting the location the of damage.

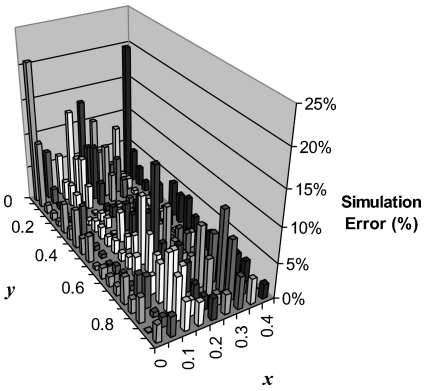

Fig. 7 Relative simulation error of NN trained with FFT of transient displacement vector at each testing point placed in midway between training data points in predicting the location the of damage.

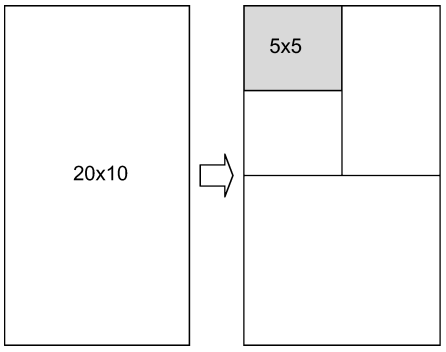

Fig. 8 Dividing 20 × 10 sections to 2 × 2 × 2 × 5 × 5 sections.

The input vector was constructed from the first 200 frequency points that include the highest mode considered in the modal superposition method for each location of displacement calculation. The size of the training input matrix was 1600 × 200. Figure 7 shows the relative error of the trained NN in simulating damage location with FFT of the transient displacement vector. It took about 1 h and 30 min to train the NN. The value of the average mean error in this case was close to that of the case where PCA of the displacement vector was used as input. However, there were more variations in the simulation error, and there were high values of error in certain points.

To select smaller number of training sets, OAs were used. The original training space is 10 × 20 and composed of 200 cases. To apply an OA of known construction to this problem, the space composed of 10 × 20 was divided into different a parameter space: 10 × 20 was divided into 2 × 2 × 2 × 5 × 5 sections as shown in Fig. 8, and an OA was applied in selecting the minimum set. Figure 9 shows the part of an OA selected in this study. The number of the set selected with this OA was half the number of the whole set. Therefore, the size of the training input matrix became 44 × 100 from 44 × 200. The training took only 7 s, whereas the NN with

	1	2	3	4	5
1	0	0	0	0	4
2	0	1	1	0	4
3	1	0	1	0	4
4	1	1	0	0	4
5	0	0	0	1	2
6	0	1	1	1	2
7	1	0	1	1	2
8	1	1	0	1	2

Fig. 9 Part of an OA for 3 factors with 2 levels, 2 factors with 5 levels, and strength 2.

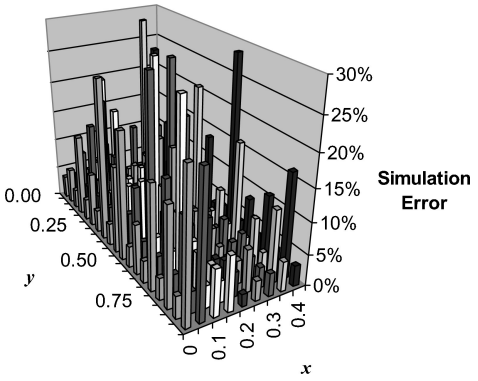

Fig. 10 Relative simulation error of NN trained with training set obtained from PCA of transient displacement vector and selection from OA at each testing point placed in midway between training data points in predicting the location the of damage.

PCA took 24 s and NN with FFT took 1 h and 30 min. Figure 10 shows the simulation errors between 2 and 29%.

Optical Medical Imaging

In the optical imaging problem, the orientation of an anomaly in a circular-shaped tissue was identified based on integrated intensity and photon mean time of flight based on the detector readings placed around the tissue as shown in Fig. 11. The property of photons that have passed through the tissue can be calculated using photon transportation theory. A good approximation to this theory is the photon diffusion equation. FEM can be readily used to solve this photon diffusion equation to obtain the property of light that went through the tissue. Two kinds of photon properties were calculated in this study. One is the time-independent integrated light intensity and the other is the photon mean time of the flight. The methods to solve these two properties followed the work of Arridge et al.[10] and Arridge and Schweiger[11] and are explained in the Appendix.

There are various kinds of source and boundary conditions in tissue optics. The Dirichlet boundary condition assumes a perfect absorbing medium surrounding the domain. The Robin boundary condition assumes a nonscattering medium surrounding the domain. The Dirichlet boundary condition was assumed in our analysis because of its ease in application.

For source conditions, two kinds of conditions are mainly used in tissue optics. One is the collimated source condition, which is represented by an isotropic point source located at a depth. The other is the diffused source condition, which assumes that an inward directed diffuse photon current is distributed over the illuminated boundary segment. The collimated source condition was assumed in our analysis.

In the numerical experiment, the dimension of the original training set for the model with 20 sources and 20 detectors was 400. When the contribution limit set was 0.075% for PMTF inputs, the dimension was reduced from 400 to 80 after the PCA. In the case of integrated intensity E, the dimension reduced to 82 from 400 when the contribution limit was set to 0.005%. As shown in Fig. 12,

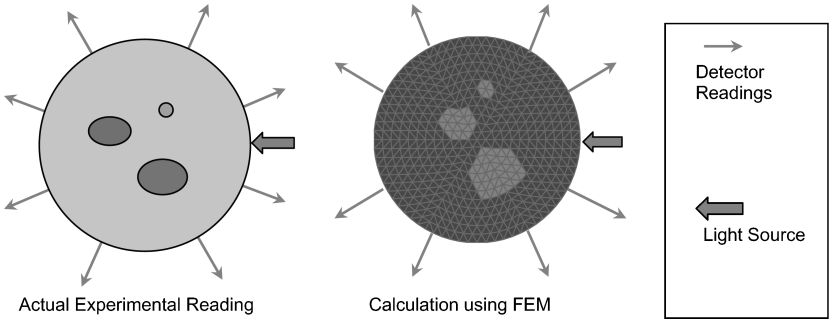

Fig. 11 Solution of direct problem.

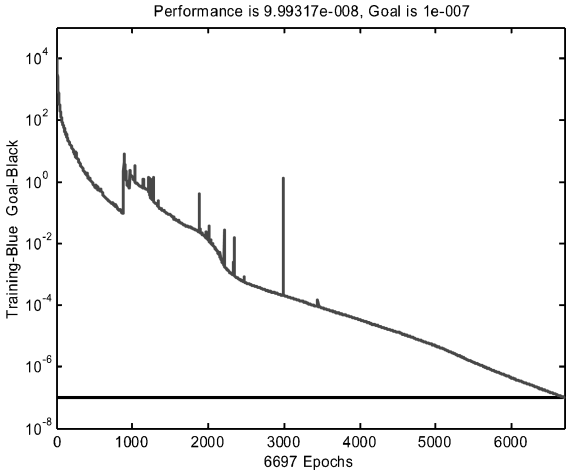

a) PMTF, 6697 epochs

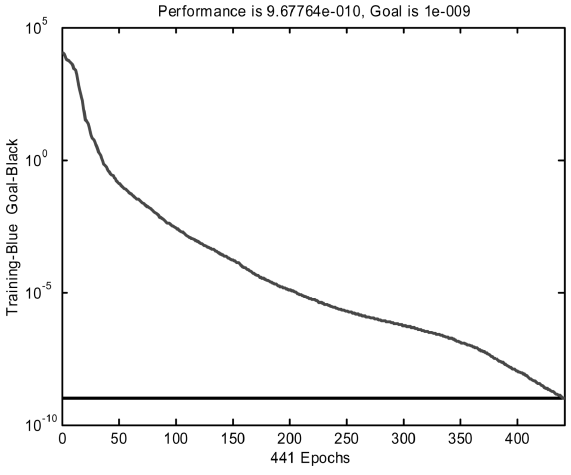

b) PMTF with PCA, 441 epochs

Fig. 12 Learning process for various sets for training inputs with and without PCA and epochs for desired degree of training.

PCA saves training time and achieves a smoother training process. Figure 13 shows the simulation error for different combinations of inputs. Among the various cases, we can see that a combined input of PMTF and E with the PCA gave the most accurate results.

Next, PCA was used in reducing the size of the training set for the element property simulation NN, whose output neurons simulate the absorption constants of each element in the FE model. The PCA reduced the size of training input from a 144×274 data set to a 72×274 data set, thereby reducing the time to train the NN by a factor of four and increasing the probability of success in the prediction of the edge of an anomaly using integrated photon intensity measurements. Figure 14a shows the convergence of the simulation error in the learning process without PCA on the training input. It did not reduce the error to less than 10^{-4} even after 5811 epochs. Figure 14b shows the convergence of simulation error in the learning

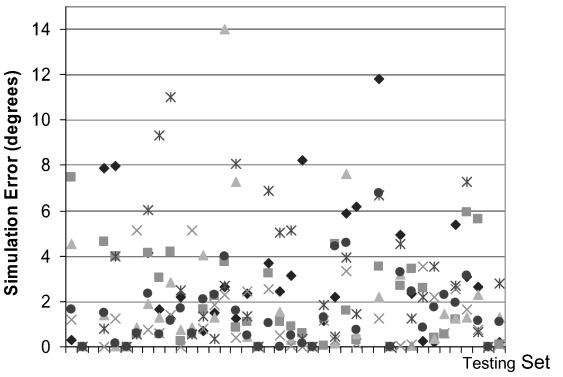

Fig. 13 Simulation error in predicting the orientation of an anomaly: ♦, PMTF; ■, PMTF and PCA; ▲, E; ×, E and PCA; ∗, PMTF and E; and ●, PMTF, E, and PCA.

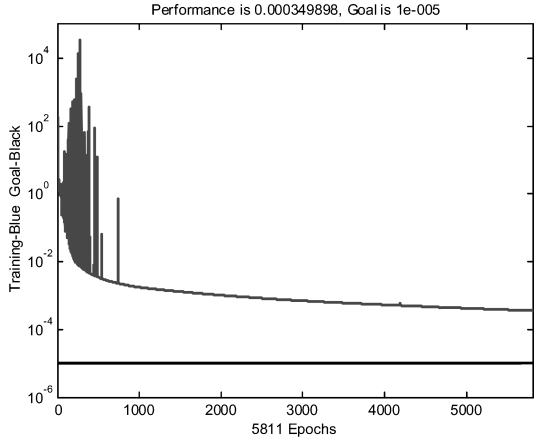

a) Training without PCA

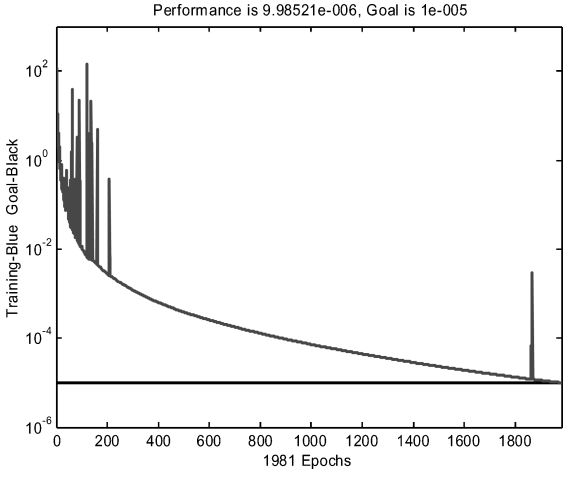

b) Training with PCA

Fig. 14 Training process of NNs to identify element properties.

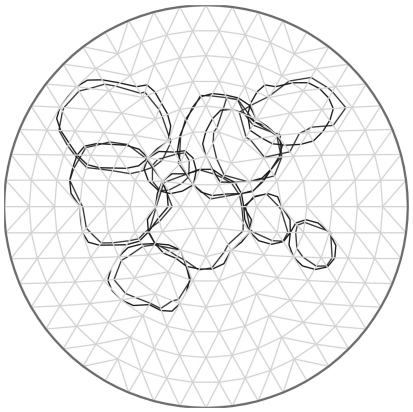

Fig. 15 Simulation of element properties for 10 cases; each case tried separately.

process with PCA. Here, we can see that it took only 1981 epochs to reduce the error below 10^{-5}. Figure 15 shows the simulated edges of the anomalies by NN. The NN trained with PCA closely identified the edge of the anomaly. In the case of the NN trained without PCA, the close prediction was 9 out of 10 testing sets.

Conclusions

PCA and OAs were used to reduce time and effort required in solving inverse problems. In the damage identification problem in a plate, it was found that the use of PCA can reduce the training time by more than hundreds of times and results in a NN that gaves an output with consistent level of error. The reason that the simulation error of NN trained with PCA data is not less than a certain level is that a certain characteristic is lost in the process of PCA, but another characteristic strengthened the consistency data with PCA. The use of PCA in an optical imaging problem gave output without a bottom limit for the simulation error. This seems to be because the characteristics of the input data are different in the two problems. Also, the use of OA reduced the time and effort required in applying NNs to solve the damage identification problem.

The code developed in the MATLAB environment that can automatically connect NASTRAN analysis to MATLAB analysis made it possible to generate enough training data for NNs in the damage identification problem. Moreover, this code has made it possible to use a highly complex NASTRAN structural model in an analysis or a design process that involves NNs and other analyses such as the mode superposition method and FFT analysis in MATLAB environment.

Appendix: Calculation of Photon Properties

The photon diffusion equation that approximates the photon transport in human tissue can be expressed as

$$\frac{1}{c_n}\frac{\partial}{\partial t}\Phi(\boldsymbol{r},t) - \nabla\cdot[D(\boldsymbol{r})\nabla\Phi(\boldsymbol{r},t)] + \mu_a(\boldsymbol{r})\Phi(\boldsymbol{r},t) = S(\boldsymbol{r},t) \quad \text{(A1)}$$

where $D(\boldsymbol{r})$ is the diffusion constant, $F(t)$ the diffusion intensity, $S(\boldsymbol{r}, t)$ the source strength, $\mu_a(\boldsymbol{r})$ the absorption coefficient, $\boldsymbol{r}$ the position, t the time, and c_n the speed of light in the medium.

The solution of this light diffusion equation is obtained by FEM using the Galerkin approach (see Ref. 10),

$$[\boldsymbol{K}(\kappa) + \boldsymbol{C}(\mu_a, c)]\,\Phi + \boldsymbol{B}\frac{\partial\Phi}{\partial t} = \boldsymbol{Q} \quad \text{(A2)}$$

$$K_{ij} = \int_\Omega \kappa(\boldsymbol{r})\nabla\psi_j(\boldsymbol{r})\cdot\nabla\psi_i(\boldsymbol{r})\,\mathrm{d}\Omega$$

$$C_{ij} = \int_\Omega \mu_a(\boldsymbol{r})c\psi_j(\boldsymbol{r})\psi_i(\boldsymbol{r})\,\mathrm{d}\Omega, \qquad B_{ij} = \int_\Omega \psi_j(\boldsymbol{r})\psi_i(\boldsymbol{r})\,\mathrm{d}\Omega$$

$$Q_j = \int_\Omega \psi_j(\boldsymbol{r})q_0(\boldsymbol{r})\,\mathrm{d}\Omega, \qquad \Phi = [\Phi_1(t), \Phi_2(t), \ldots, \Phi_D(t)]^T$$

$$\kappa(\boldsymbol{r}) = \frac{c}{3[\mu_a(\boldsymbol{r}) + \mu_s'(\boldsymbol{r})]}$$

where κ is the diffusion coefficient, μ_a the absorption coefficient, μ_s the reduced scattering coefficient, and c the speed of light.

The time-independent photon intensity is calculated as

$$\hat{\Phi}(\omega)|_{\omega=0} = \frac{1}{\sqrt{2\pi}}\int_0^\infty \Phi(t)\,\mathrm{d}t = [\boldsymbol{K}(\kappa) + \boldsymbol{C}(\mu_a, c)]^{-1}\boldsymbol{Q} \quad \text{(A3)}$$

To introduce the concept of PMTF, Mellin transform needs to be introduced. Mellin transform, which is the moment of the temporal distribution of an intensity, can be expressed as

$$\Gamma^*(s) = \int_0^\infty t^{s-1}\Gamma(t)\,\mathrm{d}t \quad \text{(A4)}$$

where Γ is a time-varying intensity.

Then, the mean time of the occurrence of the time-varying intensity shown in Fig. A1 is

$$\langle t\rangle = \frac{\int_0^\infty t\Gamma(t)\,\mathrm{d}t}{\int_0^\infty \Gamma(t)\,\mathrm{d}t} = \frac{\Gamma^*(2)}{\Gamma^*(1)} \quad \text{(A5)}$$

The definition of the Fourier transform is

$$\hat{G}(\omega) = \frac{1}{\sqrt{2\pi}}\int_{-\infty}^\infty e^{-i\omega t}g(t)\,\mathrm{d}t \quad \text{(A6)}$$

Differentiation by ω results in

$$\frac{\partial\hat{G}(\omega)}{\partial\omega} = \frac{-i}{\sqrt{2\pi}}\int_{-\infty}^\infty te^{-i\omega t}g(t)\,\mathrm{d}t, \qquad g(t) = 0, \qquad t < 0 \quad \text{(A7)}$$

When ω is zero, the Fourier transform becomes

$$\hat{G}(\omega)|_{\omega=0} = \frac{1}{\sqrt{2\pi}}\int_{-\infty}^\infty g(t)\,\mathrm{d}t \quad \text{(A8)}$$

$$\int_0^\infty g(t)\,\mathrm{d}t = \sqrt{2\pi}\hat{G}(\omega)\Big|_{\omega=0} = G^*(1) \quad \text{(A9)}$$

When ω is zero, the derivation of the Fourier transform becomes

$$\left.\frac{\partial\hat{G}(\omega)}{\partial\omega}\right|_{\omega=0} = \frac{-i}{\sqrt{2\pi}}\int_{-\infty}^\infty tg(t)\,\mathrm{d}t$$

$$\int_0^\infty tg(t)\,\mathrm{d}t = i\sqrt{2\pi}\left.\frac{\partial\hat{G}(\omega)}{\partial\omega}\right|_{\omega=0} = G^*(2) \quad \text{(A10)}$$

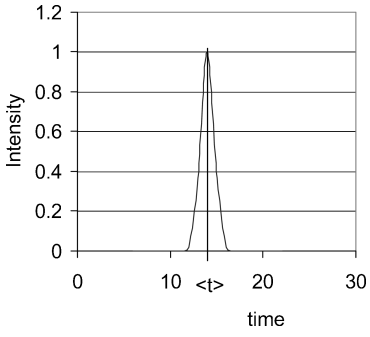

Fig. A1 Time-varying intensity; $\langle t\rangle$ is mean time of occurrence of intensity.

Therefore, the mean time of flight can be expressed with Fourier transform and its derivation as

$$\langle t\rangle = \frac{\int_0^\infty t g(t)\,\mathrm{d}t}{\int_0^\infty g(t)\,\mathrm{d}t} = \frac{G^*(2)}{G^*(1)}$$

$$= \frac{i[\partial \hat{G}(\omega)/\partial\omega]|_{\omega=0}}{\hat{G}(\omega)|_{\omega=0}} \tag{A11}$$

Taking the Fourier transform in Eq. (A2) results in

$$[\boldsymbol{K}(\kappa) + \boldsymbol{C}(\mu_a, c) + i\omega\boldsymbol{B}]\hat{\boldsymbol{\Phi}}(\omega) = \hat{\boldsymbol{Q}}(\omega) \tag{A12}$$

Differentiating with ω results in

$$[\boldsymbol{K}(\kappa) + \boldsymbol{C}(\mu_a, c) + i\omega\boldsymbol{B}]\frac{\partial\hat{\boldsymbol{\Phi}}(\omega)}{\partial\omega} + i\boldsymbol{B}\hat{\boldsymbol{\Phi}}(\omega) = \frac{\partial\hat{\boldsymbol{Q}}(\omega)}{\partial\omega} = 0 \tag{A13}$$

When Q is an impulse, its Fourier transform is a constant and the derivation is zero.

Evaluation of Eqs. (2) and (3) at $\omega = 0$ results in

$$[\boldsymbol{K}(\kappa) + \boldsymbol{C}(\mu_a, c)]\frac{\partial\hat{\boldsymbol{\Phi}}(\omega)}{\partial\omega}\bigg|_{\varpi=0} = -i\boldsymbol{B}\hat{\boldsymbol{\Phi}}(\omega)|_{\varpi=0} \tag{A14}$$

$$i\frac{\partial\hat{\boldsymbol{\Phi}}(\omega)}{\partial\omega}\bigg|_{\varpi=0} = [\boldsymbol{K}(\kappa) + \boldsymbol{C}(\mu_a, c)]^{-1}\boldsymbol{B}\hat{\boldsymbol{\Phi}}(\omega)\big|_{\varpi=0} = \Phi^*(2) \tag{A15}$$

Mean time of flight is calculated as

$$\langle t\rangle = \frac{\int_0^\infty t\Phi(t)\,\mathrm{d}t}{\int_0^\infty \Phi(t)\,\mathrm{d}t} = \frac{\Phi^*(2)}{\Phi^*(1)}$$

$$= \frac{i[\partial\hat{\Phi}(\omega)/\partial\omega]|_{\omega=0}}{\hat{\Phi}(\omega)|_{\omega=0}}$$

$$= \frac{[\boldsymbol{K}(\kappa) + \boldsymbol{C}(\mu_a, c)]^{-1}\boldsymbol{B}\hat{\Phi}(\omega)\big|_{\omega=0}}{\hat{\Phi}(\omega)|_{\omega=0}} \tag{A16}$$

Acknowledgments

This work was supported partly by the Carilion Biomedical Institute, Roanoke, Virginia, and the Optical Science and Engineering Research Center at Virginia Polytechnic Institute and State University. The authors thank the Carilion Biomedical Institute and Optical Science and Engineering Research Center for their valuable support. Thanks are also due to the Center for Healthcare Technology Development, Jeonju-si, Republic of Korea.

References

[1]Kim, Y. Y., and Kapania, R. K., "Neural Networks for Inverse Problems in Damage Identification and Optical Imaging," *AIAA Journal*, Vol. 41, No. 4, 2003, pp. 732–740.

[2]Müller, G. J., *Medical Optical Tomography: Functional Imaging and Monitoring*, SPIE Optical Engineering Press, Bellingham, WA, 1993, pp. 12–20.

[3]Arridge, S. R., "A Gradient-Based Optimization Scheme for Optical Tomography," *Optics Express*, Vol. 2, No. 6, 1997, pp. 213–226.

[4]Arridge, S. R., and Schweiger, M., "Image Reconstruction in Optical Tomography," *Philosophical Transactions of the Royal Society of London, Series B: Biological Sciences*, Vol. 352, No. 1354, 1997, pp. 717–726.

[5]Diamantaras, K. I., and Kung, S. Y., *Principal Component Neural Networks*, Wiley-Interscience, New York, 1996, pp. 44–73.

[6]Zang, C., and Imergun, M., "Structural Damage Detection Using Artificial Neural Networks and Measured FRF Data Reduced via Principal Component Projection," *Journal of Sound and Vibrations*, Vol. 242, No. 5, 2001, pp. 813–827.

[7]Hedayat, A. S., Sloane, N. J. A., and Stufken, J., *Orthogonal Arrays*, Springer, New York, 1999, pp. 199–340.

[8]Chang, C. C., Chang, T. Y. P., and Xu, Y. G., "Selection of Training Samples for Model Updating Using Neural Networks," *Journal of Sound and Vibration*, Vol. 249, No. 5, 2002, pp. 867–883.

[9]Peace, G. S., *Taguchi Methods, A Hands On Approach*, Addison–Wesley, Reading, MA, 1993.

[10]Arridge, S. R., Schweiger, M., Hiraoka, M., and Delpy, D. T., "A Finite Element Approach for Modeling Photon Transport in Tissue," *Medical Physics*, Vol. 20, No. 2, 1993, pp. 299–309.

[11]Arridge, S. R., and Schweiger, M., "Direct Calculation of the Moments of the Distribution of Photon Time of Flight in Tissue with a Finite-Element Method," *Applied Optics*, Vol. 34, No. 15, 1995, pp. 2683–2687.

S. Saigal
Associate Editor